

RECONCILING MODELS OF LUMINOUS BLAZARS WITH MAGNETIC FLUXES DETERMINED BY RADIO CORE SHIFT MEASUREMENTS

KRZYSZTOF NALEWAJKO^{1,2,3}, MAREK SIKORA^{4,5}, AND MITCHELL C. BEGELMAN^{1,6}*Draft version October 20, 2014*

ABSTRACT

Estimates of magnetic field strength in relativistic jets of active galactic nuclei (AGN), obtained by measuring the frequency-dependent radio core location, imply that the total magnetic fluxes in those jets are consistent with the predictions of the magnetically-arrested disk (MAD) scenario of jet formation. On the other hand, the magnetic field strength determines the luminosity of the synchrotron radiation, which forms the low-energy bump of the observed blazar spectral energy distribution (SED). The SEDs of the most powerful blazars are strongly dominated by the high-energy bump, which is most likely due to the external radiation Compton (ERC) mechanism. This high Compton dominance may be difficult to reconcile with the MAD scenario, unless 1) the geometry of external radiation sources (broad-line region, hot-dust torus) is quasi-spherical rather than flat, or 2) most gamma-ray radiation is produced in jet regions of low magnetization, e.g., in magnetic reconnection layers or in fast jet spines.

Keywords: galaxies: active — galaxies: jets — gamma rays: galaxies — quasars: general — radiation mechanisms: non-thermal

1. INTRODUCTION

Relativistic jets of active galactic nuclei (AGN) are launched by spinning black holes (BH) or accretion disks (Blandford & Znajek 1977; Blandford & Payne 1982). In radio galaxies and radio-loud quasars they are relativistic and reach powers comparable to or sometimes even exceeding the accretion powers (Rawlings & Saunders 1991; Ghisellini et al. 2011; Punsly 2011). Launching such powerful jets requires magnetic fluxes which cannot be developed by dynamo mechanisms in standard, radiation-dominated accretion disks (Ghosh & Abramowicz 1997). However, such fluxes are expected in the magnetically-arrested disk (MAD) scenario (Narayan et al. 2003; McKinney et al. 2012, and references therein). In this case jets are produced most likely by the Blandford-Znajek mechanism, and the required strong net magnetic flux is expected to be accumulated on the BH by the advection of magnetic fields from external regions (Sikora & Begelman 2013, and references therein). Starting as Poynting flux-dominated outflows, these jets are smoothly accelerated as they convert energy from magnetic to kinetic and their magnetization $\sigma = B'^2/(4\pi w)$, where w is the relativistic enthalpy density, drops with distance (Komissarov et al. 2007; Tchekhovskoy et al. 2009, and references therein). The jet acceleration becomes inefficient when $\sigma \lesssim 1$, from which point on, in the ideal magnetohydrodynamical (MHD) picture, σ decreases logarithmically with dis-

tance (Lyubarsky 2010). This transition between the two acceleration regimes may happen already at the distance of $10^3 R_g \sim 0.05$ pc (here $R_g = GM_{\text{bh}}/c^2$ is the gravitational radius of the black hole of mass $M_{\text{bh}} \sim 10^9 M_\odot$) (Komissarov et al. 2007).

AGN jets produce large amounts of non-thermal radiation, which is relativistically enhanced by 2 – 3 orders of magnitude in blazars, where the jets are oriented close to the line of sight (Blandford & Königl 1979). This radiation is generally thought to be produced at a distance scale $0.01 \text{ pc} < r < 10 \text{ pc}$, but in many cases it can be narrowed to $0.1 \text{ pc} < r < 1 \text{ pc}$ (see Nalewajko et al. 2014 for a recent discussion). This main emission and dissipation region is referred to as the blazar zone. Modeling of the spectral energy distributions (SED) of blazars can be used to constrain the jet composition in the blazar zone (e.g., Sikora & Madejski 2000). The most luminous blazars, belonging to the class of flat-spectrum radio quasars (FSRQs), are strongly dominated by the gamma-ray emission, which is thought to be produced by the external-radiation-Comptonization (ERC) mechanism (Dermer et al. 1992; Sikora et al. 1994, 2009), the efficiency of which depends on the energy density of external radiation fields, mainly the broad emission lines (BEL) and the thermal radiation of the dusty torus. The very high apparent gamma-ray luminosities of FSRQs, at times exceeding $L_\gamma \sim 10^{48} \text{ erg s}^{-1}$ (Abdo et al. 2011), call for very high total jet powers $L_j \sim 10^{46-47} \text{ erg s}^{-1}$ and high radiative efficiencies $\eta = L_\gamma/(\Gamma_j^2 L_j) \sim 0.1$ (Nemmen et al. 2012), where $\Gamma_j \sim 20$ is the jet Lorentz factor. On the other hand, most of the infrared/optical emission of blazars is due to the synchrotron mechanism, the efficiency of which depends on the local magnetic field strength. Observations of blazars with high dominance of the ERC component over synchrotron emission place strong constraints on σ within the blazar zone, which we discuss in Section 2.

Recently, the magnetic field strength scaled to the

¹ JILA, University of Colorado and National Institute of Standards and Technology, 440 UCB, Boulder, CO 80309, USA

² Kavli Institute for Particle Astrophysics and Cosmology, SLAC National Accelerator Laboratory, Stanford University, 2575 Sand Hill Road M/S 29, Menlo Park, CA 94025, USA; knalew@stanford.edu

³ NASA Einstein Postdoctoral Fellow

⁴ Nicolaus Copernicus Astronomical Center, Bartycka 18, 00-716 Warsaw, Poland

⁵ JILA Visiting Fellow

⁶ Department of Astrophysical and Planetary Sciences, University of Colorado, 391 UCB, Boulder, CO 80309, USA

distance of 1 pc was estimated for a large sample of blazars and radio galaxies by using the core-shift technique (Pushkarev et al. 2012). In this technique, the position of the radio core, assumed to be a photosphere due to the synchrotron self-absorption process (Blandford & Königl 1979), is measured in relation to sharp optically thin jet features as a function of observing frequency (Lobanov 1998). These magnetic field values were used to estimate the magnetic fluxes of jets Φ_j , which were compared to the theoretical magnetic fluxes threading the black holes Φ_{bh} as predicted by the MAD scenario (Zamaninasab et al. 2014). The close agreement between Φ_j and Φ_{bh} strongly supports the MAD scenario for production of powerful AGN jets. In Section 3, we show that this is equivalent to a relation $L_B \sim L_d$ between the magnetic jet power and accretion disk luminosity.

We identified a possible tension between the magnetic field strengths estimated from core-shift measurements, and the magnetic field strengths estimated from modeling the emission of the most Compton-dominated FSRQs. The latter tend to be lower by factor ~ 3 , therefore, in Section 4 we consider dissipation sites that involve lower than average local magnetic field strengths: 1) magnetic reconnection layers, and 2) weakly-magnetized jet spines. We also emphasize the importance of the geometric distribution of external radiation sources, in particular that a flat geometry of the broad-line region (BLR) and/or the dusty torus makes the problem much worse. Our main results are summarized in Section 5.

2. HIGH COMPTON DOMINANCE IN FSRQs

The SEDs of FSRQs are strongly dominated by the high-energy component peaking in the 10-100 MeV range, which is most naturally explained by the ERC model (Sikora et al. 2009). We define the Compton dominance parameter $q = L_{ERC}/L_{syn}$, where L_{ERC} and L_{syn} are the apparent luminosities of the ERC and synchrotron components, respectively, at their spectral peaks. Numerous observations indicate that quite often $q \gtrsim 10$ for the brightest blazars (Abdo et al. 2010; Arshakian et al. 2012; Giommi et al. 2012).

On the other hand, if the ERC and synchrotron components are produced by the same population of electrons,⁷ we can write $q \simeq u'_{ext}/u'_B$, where u'_{ext} and u'_B are the energy densities of the external radiation field and the magnetic field in the jet co-moving frame, respectively. The external radiation density can be parametrized as $u'_{ext} = \zeta \Gamma^2 L_d / (4\pi cr^2)$, where ζ is a dimensionless parameter representing the details of reprocessing and beaming of the external radiation (see below), Γ is the Lorentz factor of the emitting region, L_d is the accretion disk luminosity, and r is the distance of the emitting region from the supermassive black hole. The magnetic energy density can be related to the jet magnetic power $L_B = 2\pi R^2 \Gamma^2 u'_B c$, where $R = \theta_j r$ is the jet radius, and θ_j is the half-opening angle of the jet. Gathering these

relations together, we obtain the following constraint:

$$q = \left(\frac{\zeta}{0.005} \right) \left(\frac{\Gamma}{20} \right)^2 (\Gamma \theta_j)^2 \left(\frac{L_d}{L_B} \right). \quad (1)$$

Written in such form, the above equation suggests the typical parameter values that we adopt as the starting point for further discussion.

The parameter $\zeta = \xi g_u$ includes the traditional covering factor ξ , and the geometric factor g_u (Sikora et al. 2013). The covering factor determines the total luminosity of the reprocessed accretion disk radiation, e.g., $L_{BLR} = \xi_{BLR} L_d$. Typically, it is assumed that $\xi \simeq 0.1$, although there are many indications that it can be as high as $\xi \sim 0.4$ both for the BLR (Dunn et al. 2007; Gaskell 2009), and for the dusty tori (Roseboom et al. 2013; Wilkes et al. 2013). The geometric factor depends on the geometric distribution of the reprocessing medium, and on the radial stratification of the covering factor. As we show in the Appendix, even for a spherical distribution $g_u < 0.7$, and for flattened distributions $g_u < 0.1$. Recently, there has been increasing interest in flattened distributions of the BLR (Tavecchio & Ghisellini 2012), motivated mainly by observations of rapidly variable VHE emission from quasars (Aleksić et al. 2011), and supported by direct observations (Vestergaard et al. 2000; Decarli et al. 2011). The half-opening angle of the dusty tori is being estimated at $\sim 30^\circ$ (Wilkes et al. 2013). Assuming that $g_u = \xi = 0.1$, we can expect that ζ can be as low as 0.01. However, in the case of a quasi-spherical reprocessing medium with high covering factor, we may expect $\xi \simeq 0.4$ and $g_u \simeq 0.5$, and hence $\zeta \simeq 0.2$. High values of q may thus require the presence of a dense, quasi-spherical medium reprocessing the central AGN radiation.

The Lorentz factors Γ of blazar jets can be estimated from interferometric observations of apparent superluminal motions of radio features. Typical values for FSRQs are $10 < \Gamma < 40$ (Hovatta et al. 2009). The jet collimation parameter $\Gamma \theta_j$ should not exceed unity on both theoretical (Komissarov et al. 2009) and observational (Jorstad et al. 2005; Pushkarev et al. 2009) grounds. Therefore, it is very unlikely that we could obtain $q > 10$ by increasing either the Lorentz factor or the collimation parameter.

Finally, the parameter q can be increased by decreasing the magnetic jet power so that $L_B < L_d$. If the jets are significantly magnetized, with $\sigma \simeq L_B / (L_j - L_B) > 1$, we would expect that $L_B \lesssim L_j$, where L_j is the total jet power. Observational evidence suggests that for the most powerful jets $L_j \sim \dot{M} c^2 > L_d$ (see Section 1). This would be also consistent with the MAD scenario, in which it was demonstrated numerically that $L_j \gtrsim \dot{M} c^2$ (Tchekhovskoy et al. 2011). As we show in the next section, the requirement that $L_B \sim L_d$ is equivalent to the relation between the two magnetic fluxes $\Phi_j \sim \Phi_{bh}$ (Zamaninasab et al. 2014), therefore increasing q by decreasing L_B globally means a departure from the MAD scenario (in addition to departing from the core-shift measurements). However, one can still consider a local decrease in the magnetic field strength in order to obtain a high q (see Section 4).

⁷ Statistically, blazars show significant correlation between the gamma-ray and optical fluxes (e.g., Cohen et al. 2014). However, there are cases of poor correlation (e.g., Chatterjee et al. 2013), in which one needs to consider multiple emitting regions. In such cases, one can focus on the main gamma-ray emitting region and place upper limits on the co-spatial synchrotron emission.

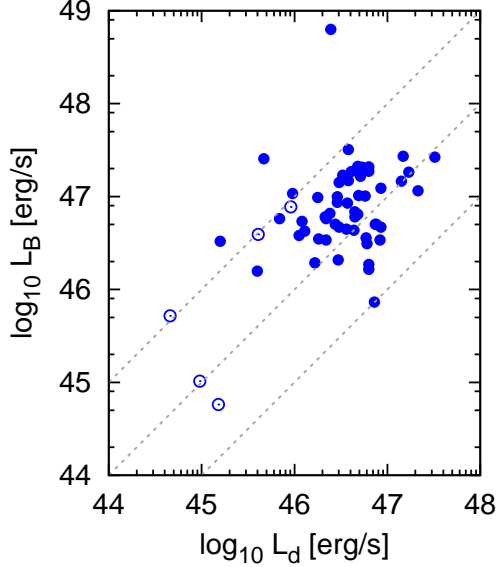


Figure 1. Distribution of the accretion disk luminosity L_d vs. the magnetic jet power L_B for the sample of blazars (FSRQs – *solid points*; BL Lacs – *empty points*) compiled by Zamaninasab et al. (2014). It is assumed that $\Gamma\theta_j = 1$.

3. JET MAGNETIC FIELDS FROM CORE-SHIFT MEASUREMENTS

In this section we analyze the sample of blazars compiled by Zamaninasab et al. (2014), for which magnetic field estimates B'_{1pc} from core-shift measurements are available (Pushkarev et al. 2012), as well as accretion disk luminosities L_d , and black hole masses M_{bh} .

First, we estimate the magnetic jet power as $L_B \simeq (c/4)(1 \text{ pc})^2 B'^2_{1pc} (\Gamma\theta_j)^2$. In Figure 1, we show the distribution of L_B vs. L_d for the case of $\Gamma\theta_j = 1$. We note a substantial scatter in the L_B values, most of them falling in the range $0.2 < L_B/L_d < 20$. The sources with $L_B < L_d$ may have $q > 1$, according to Eq. 1. However, very few sources in this sample can have $q > 10$ solely due to the low value of L_B/L_d . As the magnetic jet power is a steep function of the jet collimation parameter $\Gamma\theta_j$, allowing for $\Gamma\theta_j < 1$ can substantially reduce L_B . However, since $q \propto (\Gamma\theta_j)^2/L_B$ (Eq. 1), the Compton dominance would not be affected by adopting a different value of $\Gamma\theta_j$.

The correlation between L_B and L_d is much worse than the correlation between the two magnetic fluxes Φ_j and Φ_{bh} identified by Zamaninasab et al. (2014). Those magnetic fluxes can be written as:

$$\begin{aligned} \Phi_j &\simeq 8\pi(\Gamma\theta_j)f(a)R_g B'_{1pc}(1 \text{ pc}) \propto (\Gamma\theta_j)f(a)L_B^{1/2}M_{bh}(2) \\ \Phi_{bh} &\simeq 50R_g \left(\frac{L_d}{\eta c}\right)^{1/2} \propto L_d^{1/2}M_{bh}, \end{aligned} \quad (3)$$

where η is the radiative efficiency of the accretion disk, $f(a) = [1 + (1 - a^2)^{1/2}]/a$, and a is the dimensionless black hole spin. The very good correlation between the magnetic fluxes for $\Gamma\theta_j = 1$, $a = 1$, and $\eta = 0.4$ can be partly explained by the fact that both fluxes are proportional to the black hole mass M_{bh} . Because of the wide range of M_{bh} (about 3 orders of magnitude, $10^7 - 10^{10} M_\odot$),

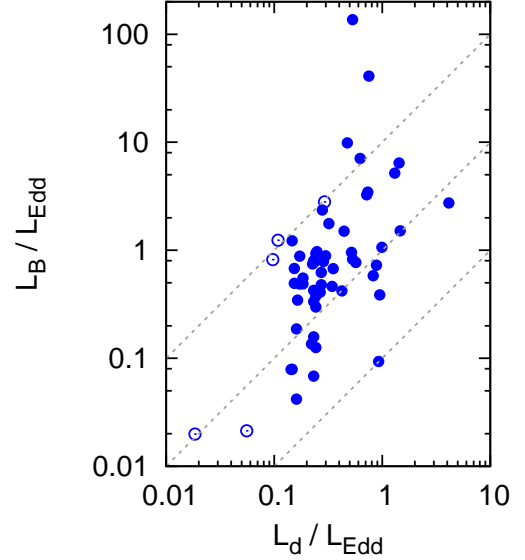


Figure 2. Same as in Figure 1, but with both quantities scaled to the Eddington luminosity L_{Edd} .

the relatively poor correlation between L_B and L_d is efficiently stretched along the lines of constant L_B/L_d . Also, since $\Phi_j/\Phi_{bh} \simeq (L_B/L_d)^{1/2}$, the scatter between the Φ_j/Φ_{bh} values is smaller than the scatter between the L_B/L_d values.

In Figure 2, we show the relation between L_B/L_{Edd} and L_d/L_{Edd} , where $L_{Edd} = 1.6 \times 10^{38} (M_{bh}/M_\odot) \text{ erg s}^{-1}$ is the Eddington luminosity. We note that the blazars in the sample compiled by Zamaninasab et al. (2014) occupy a narrow range of Eddington luminosity ratios, with $0.1 \lesssim L_d/L_{Edd} \lesssim 2$. All sources in the sample must have prominent broad emission lines in order to calculate both L_d and M_{bh} . Because of this selection effect, effectively we have $L_d \propto M_{bh}$, $L_B \propto M_{bh}$, and the magnetic fluxes scale as $\Phi_j \simeq \Phi_{bh} \propto M_{bh}^{3/2}$.

4. LOW-MAGNETIZATION DISSIPATION SITES

We consider two potential mechanisms for obtaining reduced local magnetic field strengths in jets of typical magnetization $\sigma \sim 1$: one associated with reconnection layers and one related to the radial structure of magnetic fields across the jets. Magnetic reconnection events are likely to be triggered in mildly relativistic turbulent plasma which is expected to be driven by current-driven instabilities (Begelman 1998), while stratification of the toroidal magnetic component across the jet may result from balancing the magnetic stresses by the pressure of protons heated, e.g., by internal shocks.

4.1. Reconnection layers

Magnetic reconnection was proposed as an alternative dissipation mechanism for powering rapid high-amplitude gamma-ray flares in blazars (Giannios et al. 2009). Efficient reconnection may reduce the local magnetic field strength by factor $\gtrsim 3$, which is necessary in order to achieve high Compton dominance $q > 10$, if the guide magnetic field component is more than 3 times smaller than the antiparallel magnetic field component.

Then, provided that magnetic energy released in the reconnection process is equally shared between protons and electrons (Melzani et al. 2014), the electrons are injected with average random Lorentz factor $\bar{\gamma}_e \sim (m_p/m_e)\sigma \sim 10^3$. For $\sigma \sim 1$, these electrons can Comptonize external soft photons up to energy $h\nu_{\text{ERC}} \simeq (\Gamma/20)^2 (h\nu_{\text{ext}}/10 \text{ eV})$ GeV. In the case of ERC(BLR), this is ~ 100 times larger than the energy of photons at typical γ -ray luminosity peaks, and in the case of ERC(IR) — ~ 3 times larger.

In order to reconcile these energies with the peak location, it is necessary to postulate an e^+e^- pair content — again assuming an equal energy partition between electrons and protons — $n_e/n_p \sim 100$ for ERC(BLR) and $n_e/n_p \sim 3$ for ERC(HDR), where $n_e = n_{e^+} + n_{e^-}$. Noting that the efficiency of pair production at the characteristic distance scale of the BLR and beyond is very low (the production of pairs by absorption of the γ -rays by the UV photons requires an extension of the γ -ray spectra above ~ 30 GeV), such pairs must be produced at much lower distances, close to the jet base, where they can result from the absorption of the γ -rays by the X-rays produced in the accretion disk corona. The significant pair content required in the reconnection scenario may explain why in the jet terminal shocks associated with radio-lobe hot spots, the observed low-energy break in the electron energy distribution is much lower than predicted by relativistic proton-electron shocks (Stawarz et al. 2007; Godfrey & Shabala 2013, and references therein).

4.2. Central core/spine

If the jet has a lateral structure with a weakly magnetized core/spine (Ghisellini et al. 2005) with $\sigma \sim 0.1$, and particles are accelerated by internal mildly relativistic shocks, then the average energy gained by protons and electrons (if shared equally) will be $\sim \eta_{\text{diss}} m_p c^2 / 2$. For a typical efficiency of energy dissipation in mildly relativistic shocks $\eta_{\text{diss}} \sim 0.1$ (see Spada et al. 2001 for the internal shocks, and Nalewajko & Sikora 2009 for the reconfinement shocks) this gives $\bar{\gamma}_e \sim 100$. Such electrons boost external photons up to $\sim 40(\Gamma/20)^2 (h\nu_{\text{ext}}/10 \text{ eV})$ MeV, which is roughly consistent with the location of the γ -ray spectral peaks.

5. CONCLUSIONS

Magnetic fluxes Φ_j derived by measurements of radio core shifts in blazars (Pushkarev et al. 2012) are consistent with the maximum magnetic fluxes Φ_{bh} predicted by the MAD model to thread the BH (Zamaninasab et al. 2014). As we showed in Section 3, this is equivalent to the statement that magnetic jet power L_B is comparable to the accretion disk luminosity L_d , which for total jet power $L_j \sim L_d$ implies typical jet magnetizations $\sigma \sim 1$. However, as we showed in Section 2, even in the case of a geometrically thick distribution of external radiation sources, significantly lower magnetization values are required by radiation models of FSRQs in order to reproduce the high ratios q of γ -ray to synchrotron luminosities.

This inconsistency can be resolved by noting that blazar jets need not be magnetically homogeneous and uniform across the jet as commonly assumed. As discussed in Section 4, in realistic jet models there may exist regions with lower magnetization. They can be generated

by reconnection driven in mildly relativistic turbulence. They may also be associated with jet cores filled with hot protons heated by internal shocks. In both cases high values of q are achievable, and the energy of γ -ray luminosity peaks can be reproduced — in the shock scenario with a proton-electron plasma, and in the reconnection scenario with significant pair content.

We also tentatively considered a possibility that the jet magnetic fields obtained from the radio core-shift measurements are overestimated. This could be the case if the radio cores are not photospheres due to the synchrotron self-absorption process, but rather they are due to a low-energy break in the electron distribution function. This idea will be developed in a future study.

We thank the reviewers and Andrzej Zdziarski for helpful comments on the manuscript. M.S. thanks the JILA Fellows for their hospitality during the early stages of this project. This project was partly supported by the NASA Fermi Guest Investigator program, NASA Astrophysics Theory Program grant NNX14AB375, and Polish NCN grant DEC-2011/01/B/ST9/04845. K.N. was supported by NASA through Einstein Postdoctoral Fellowship grant number PF3-140130 awarded by the Chandra X-ray Center, which is operated by the Smithsonian Astrophysical Observatory for NASA under contract NAS8-03060.

APPENDIX

GEOMETRICAL CORRECTION TO THE EXTERNAL RADIATION DENSITY

In Section 2, we parametrize the energy density of the external radiation fields, using a geometrical correction factor g_u , which was first introduced in Sikora et al. (2013). Given a particular geometrical model of the distribution of the medium producing the external radiation, we can integrate the external energy density $u'_{\text{ext}}(r)$ along the jet in the co-moving frame, taking into account the exact distance and beaming factor for each volume element of the medium. Then, we calculate $g_u = 4\pi cr^2 u'_{\text{ext}} / (\xi \Gamma^2 L_d)$.

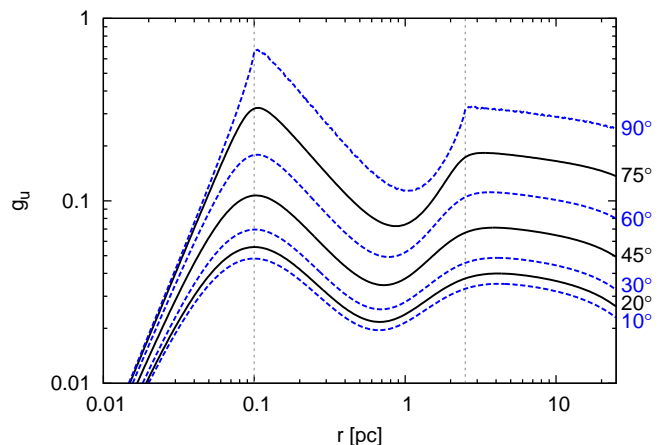


Figure 3. The dependence of the geometrical correction factor g_u for the external radiation density on the location r along the jet and on the half-opening angle α_{max} (its values for each curve are marked along the right edge) of the radiation source measured with respect to the accretion disk plane.

We adopt here a specific geometry of the reprocessing medium (either BLR or the dusty torus), presented in Appendix A of Nalewajko et al. (2014). The optical depth gradient $d\tau/dr$ is assumed to scale like r^{-2} for the BLR, and roughly like r^{-1} for the dusty torus. We also adopt the covering factors $\xi_{\text{BLR}} = \xi_{\text{IR}} = 0.1$, and typical values for the inner radii r_{BLR} and r_{IR} of the BLR and the torus, respectively, from Sikora et al. (2009). The main variable is the half-opening angle α_{max} of the medium measured from the accretion disk plane.

In Figure 3, we show the functions $g_u(r)$ for several values of α_{max} . We find that close to the characteristic radii $g_u \simeq 0.04$ for $\alpha_{\text{max}} = 10^\circ$, $g_u \simeq 0.08$ for $\alpha_{\text{max}} = 45^\circ$, and $g_u \simeq 0.2$ for $\alpha_{\text{max}} = 75^\circ$. This indicates that widely different geometries of the reprocessing medium may change g_u , and thus q , by a factor ~ 5 .

REFERENCES

- Abdo, A. A., Ackermann, M., Agudo, I., et al. 2010, *ApJ*, 716, 30
 Abdo, A. A., Ackermann, M., Ajello, M., et al., 2011, *ApJ*, 733, L26
 Aleksić, J., et al., 2011, *ApJ*, 730, L8
 Arshakian, T. G., León-Tavares, J., Böttcher, M., et al. 2012, *A&A*, 537, A32
 Begelman, M. C., 1998, *ApJ*, 493, 291
 Blandford, R. D., Königl, A., 1979, *ApJ*, 232, 34
 Blandford, R. D., & Payne, D. G., 1982, *MNRAS*, 199, 883
 Blandford, R. D., & Znajek, R. L., 1977, *MNRAS*, 179, 433
 Chatterjee, R., Fossati, G., Urry, C. M., et al. 2013, *ApJ*, 763, L11
 Cohen, D. P., Romani, R. W., Filippenko, A. V., et al. 2014, *arXiv:1404.5967*
 Decarli, R., Dotti, M., & Treves, A. 2011, *MNRAS*, 413, 39
 Dermer, C. D., Schlickeiser, R., & Mastichiadis, A., 1992, *A&A*, 256, L27
 Dunn, J. P., Crenshaw, D. M., Kraemer, S. B., & Gabel, J. R. 2007, *AJ*, 134, 1061
 Gaskell, C. M. 2009, *NewAR*, 53, 140
 Ghisellini, G., Tavecchio, F., & Chiaberge, M., 2005, *A&A*, 432, 401
 Ghisellini, G., Tagliaferri, G., Foschini, L., et al. 2011, *MNRAS*, 411, 901
 Ghosh, P., & Abramowicz, M. A. 1997, *MNRAS*, 292, 887
 Giannios, D., Uzdensky, D. A., & Begelman, M. C. 2009, *MNRAS*, 395, L29
 Giommi, P., Polenta, G., Lähteenmäki, A., et al. 2012, *A&A*, 541, A160
 Godfrey, L. E. H., & Shabala, S. S. 2013, *ApJ*, 767, 12
 Hovatta, T., Valtaoja, E., Tornikoski, M., Lähteenmäki, A., 2009, *A&A*, 494, 527
 Jorstad, S. G., Marscher, A. P., Lister, M. L., 2005, *AJ*, 130, 1418
 Komissarov, S. S., Barkov, M. V., Vlahakis, N., Königl, A., 2007, *MNRAS*, 380, 51
 Komissarov S. S., Vlahakis N., Königl A., Barkov M. V., 2009, *MNRAS*, 394, 1182
 Lobanov, A. P. 1998, *A&A*, 330, 79
 Lyubarsky, Y. E. 2010, *MNRAS*, 402, 353
 McKinney, J. C., Tchekhovskoy, A., & Blandford, R. D. 2012, *MNRAS*, 423, 3083
 Malzani, M., Walder, R., Folini, D. et al. 2014, *arXiv:1405.2938*
 Nalewajko, K., Sikora, M., 2009, *MNRAS*, 392, 1205
 Nalewajko, K., Begelman, M. C., & Sikora, M. 2014, *ApJ*, 789, 161
 Narayan, R., Igumenshchev, I. V., & Abramowicz, M. A. 2003, *PASJ*, 55, L69
 Nemmen, R. S., Georganopoulos, M., Guiriec, S., et al. 2012, *Science*, 338, 1445
 Punsly, B. 2011, *ApJ*, 728, L17
 Pushkarev, A. B., Kovalev, Y. Y., Lister, M. L., Savolainen, T., 2009, *A&A*, 507, L33
 Pushkarev, A. B., Hovatta, T., Kovalev, Y. Y., et al. 2012, *A&A*, 545, A113
 Rawlings, S., & Saunders, R. 1991, *Nature*, 349, 138
 Roseboom, I. G., Lawrence, A., Elvis, M., et al. 2013, *MNRAS*, 429, 1494
 Sikora, M., & Begelman, M. C. 2013, *ApJ*, 764, L24
 Sikora, M., & Madejski, G. 2000, *ApJ*, 534, 109
 Sikora, M., Begelman, M. C., & Rees, M. J., 1994, *ApJ*, 421, 153
 Sikora, M., Stawarz, L., Moderski, R., Nalewajko, K., & Madejski, G. M., 2009, *ApJ*, 704, 38
 Sikora, M., Janiak, M., Nalewajko, K., Madejski, G. M., & Moderski, R. 2013, *ApJ*, 779, 68
 Spada, M., Ghisellini, G., Lazzati, D., & Celotti, A., 2001, *MNRAS*, 325, 1559
 Stawarz, L., Cheung, C. C., Harris, D. E., & Ostrowski, M. 2007, *ApJ*, 662, 213
 Tavecchio, F., & Ghisellini, G. 2012, *arXiv:1209.2291*
 Tchekhovskoy, A., McKinney, J. C., & Narayan, R. 2009, *ApJ*, 699, 1789
 Tchekhovskoy, A., Narayan, R., McKinney, J. C., 2011, *MNRAS*, 418, L79
 Vestergaard, M., Wilkes, B. J., & Barthel, P. D. 2000, *ApJ*, 538, L103
 Wilkes, B. J., Kuraszkiewicz, J., Haas, M., et al. 2013, *ApJ*, 773, 15
 Zamaninasab, M., Clausen-Brown, E., Savolainen, T., & Tchekhovskoy, A. 2014, *Nature*, 510, 126